

## 2-DEOXYRIBOSE RADICALS IN THE GAS PHASE AND AQUEOUS SOLUTION. TRANSIENT INTERMEDIATES OF HYDROGEN ATOM ABSTRACTION FROM 2-DEOXYRIBOFURANOSE

Luc A. VANNIER<sup>1</sup>, Chunxiang YAO<sup>2</sup> and František TUREČEK<sup>3,\*</sup>

*Department of Chemistry, Bagley Hall, Box 351700, University of Washington, Seattle, WA 98195-1700, U.S.A.; e-mail: <sup>1</sup> lav774@u.washington.edu, <sup>2</sup> yao2002@u.washington.edu, <sup>3</sup> turecek@chem.washington.edu*

Received May 13, 2005

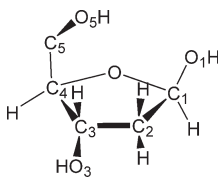
Accepted July 12, 2005

A computational study at correlated levels of theory is reported to address the structures and energetics of transient radicals produced by hydrogen atom abstraction from C-1, C-2, C-3, C-4, C-5, O-1, O-3, and O-5 positions in 2-deoxyribofuranose in the gas phase and in aqueous solution. In general, the carbon-centered radicals are found to be thermodynamically and kinetically more stable than the oxygen-centered ones. The most stable gas-phase radical, 2-deoxyribofuranos-5-yl (5), is produced by H-atom abstraction from C-5 and stabilized by an intramolecular hydrogen bond between the O-5 hydroxy group and O-1. The order of radical stabilities is altered in aqueous solution due to different solvation free energies. These prefer conformers that lack intramolecular hydrogen bonds and expose O-H bonds to the solvent. Carbon-centered deoxyribose radicals can undergo competitive dissociations by loss of H atoms, OH radical, or by ring cleavages that all require threshold dissociation or transition state energies  $>100 \text{ kJ mol}^{-1}$ . This points to largely non-specific dissociations of 2-deoxyribose radicals when produced by exothermic hydrogen atom abstraction from the saccharide molecule. Oxygen-centered 2-deoxyribose radicals show only marginal thermodynamic and kinetic stability and are expected to readily fragment upon formation.

**Keywords:** Carbohydrates; Hydrogen abstraction; Conformation analysis; DNA oxidative damage; Radiolysis; Ab initio calculations; Radical stability.

Radical intermediates are known to play a critical role in the degradation of nucleic acids caused by high-energy particles in the complex process of radiation damage<sup>1</sup>. Both the nucleobase residues and the 2-deoxyribose backbone have been shown to be attacked by reactive species formed by irradiation or pulse radiolysis, as supported by isolation of several stable products of radiation damage<sup>2</sup>. While a number of nucleobase radicals have been detected by electron paramagnetic resonance (EPR) spectroscopy after in situ radiolysis of nucleosides and nucleotides, detection of transient saccharide radicals faced experimental difficulties with signal detection and assign-

ment<sup>3</sup>. This has spurred several computational studies of model saccharide radicals that were mainly focused on obtaining structures and hyperfine splitting constants to aid interpretation of EPR spectra. The previous computational studies mainly dealt with truncated models of 2'-deoxyribonucleosides. Miaskiewicz and Osman reported Møller–Plesset level calculations for a 2-deoxyribofuranose derivative with an amino group at C-1 and no substituent at C-5<sup>4</sup>. Colson and Sevilla reported Hartree–Fock level calculations for 1,2-dideoxyribose-3,5-diphosphate and 2-deoxyribose-1-amino-3,5-diphosphate<sup>5</sup>. In a more recent study, Wetmore, Boyd, and Eriksson studied 1-amino-2-deoxyribofuranose and 2-methyltetrahydrofuran-3-ol as simple models of 2-deoxyribofuranose<sup>6</sup>. The common feature of these model compounds was that they adopted the furanose ring conformations that are typical of the 2-deoxyribofuranose ring in DNA, e.g., the envelope C-3'-*endo* (<sup>3</sup>*E*) and C-2'-*endo* (<sup>2</sup>*E*) conformations. For the nomenclature of furanose ring conformations and pseudorotation, see ref.<sup>7</sup> However, radicals derived from the parent saccharide, 2-deoxyribose, have not been studied so far.



We have recently reported joint experimental and computational studies of 2-hydroxytetrahydrofuran-2-yl<sup>8</sup> and 3-hydroxytetrahydrofuran-3-yl<sup>9</sup> radicals that were generated by femtosecond electron transfer to the respective cations in the gas phase. The radicals were found to dissociate readily by hydrogen atoms loss and ring cleavage that were identified by isotope labeling and product analysis. The present study extends the previous ones in addressing the structures and dissociation energies of carbon- and oxygen-centered radicals derived by hydrogen atom abstraction from 2-deoxyribofuranose. A computational approach is warranted by the structural ambiguity of 2-deoxyribose that is known to exist as a pyranose in a crystal<sup>10</sup> and may produce a mixture of pyranose and furanose structures when transferred to aqueous solution or the gas phase.

## COMPUTATIONAL METHODS

Standard *ab initio* and density functional theory calculations were performed using the Gaussian 03 suite of programs<sup>11</sup>. Geometries were opti-

mized with Becke's hybrid functional (B3LYP)<sup>12</sup> using the 6-31+G(d,p) basis set. The optimized structures for most relevant species are shown in Figs 1–5. Complete geometries in the Cartesian coordinate format can be obtained from the corresponding author upon request. The same level of theory was used for frequency analysis to characterize local energy minima (all real frequencies) and transition states as first-order saddle points (one imaginary frequency). Improved energies were obtained by single-point calculations using the B3LYP and Møller–Plesset theory<sup>13</sup> truncated at second order (MP2, frozen core) and the larger triple- $\zeta$  split-valence 6-311+G(2df,p) and 6-311++G(3df,2p) basis sets furnished with multiple shells of polarization functions at C, O, and H and diffuse functions at C, O (for the former basis set), and C, O, and H (for the latter basis set). Spin unrestricted formalism (UB3LYP and UMP2) was used for radicals. Spin contamination was negligible in UB3LYP calculations where the expectation values of the spin operator were  $\langle S^2 \rangle \leq 0.754$ . Spin contamination in the UMP2 calculated energies was also modest,  $\langle S^2 \rangle \leq 0.764$ , and was treated by the standard spin annihilation procedure<sup>14</sup> which reduced  $\langle S^2 \rangle$  to 0.750. The B3LYP and spin-projected MP2 single point energies were averaged according to the previously reported B3-PMP2 scheme<sup>15</sup> that has been shown to achieve improved accuracy at the level of highly correlated composite ab initio methods by cancelling small errors inherent to the B3LYP and MP2 approximations<sup>16,17</sup>. The B3-PMP2 energies were used to calculate relative energies that were corrected for zero-point vibrational contributions. The reported relative energies thus correspond to 0 K unless stated otherwise. Enthalpy corrections and entropies were calculated from B3LYP/6-31+G(d,p) harmonic frequencies and moments of inertia within the rigid rotor-harmonic oscillator approximation. Solvation energies in a polar dielectric corresponding to water were calculated using the refined polarizable continuum model (PCM)<sup>18</sup>. Geometries were fully reoptimized with PCM and B3LYP/6-31+G(d,p) using standard parameters (water dielectric constant,  $K = 78.39$ , and van der Waals atomic radii) included in Gaussian 03<sup>11</sup>. The hydration free energy of the hydrogen atom ( $13.5 \text{ kJ mol}^{-1}$ ) was taken from the work of Gai and Garrett<sup>19</sup>.

## RESULTS AND DISCUSSION

*Bond Dissociation Energies in 2-Deoxyribofuranose*

2-Deoxyribofuranose is calculated to adopt two puckered conformations (Fig. 1). The first one (**I**) is a C-2-*exo* envelope ( ${}_2E$ ) that shows a weak hydrogen bond between O-5 and H-O-1 at 2.350 Å. The other (**II**) is a C-4-*endo* envelope ( ${}_4E$ ) that shows a stronger hydrogen bond between O-5 and H-O-1 at 1.985 Å. Structures **I** and **II** are nearly isoenergetic at all levels of theory, e.g.,  $\Delta H_{g,298}^{\circ}(\mathbf{I} \rightarrow \mathbf{II}) = -0.8 \text{ kJ mol}^{-1}$  and  $\Delta G_{g,298}^{\circ}(\mathbf{I} \rightarrow \mathbf{II}) = 0.3 \text{ kJ mol}^{-1}$  from B3-MP2/6-311++G(3df,2p). Both **I** and **II** are less stable than the canonical chair form of 2-deoxy- $\alpha$ ,D-ribofuranose (**III**). From the calculated  $\Delta G_{g,298}^{\circ}(\mathbf{I} \rightarrow \mathbf{III}) = -13.3 \text{ kJ mol}^{-1}$  one obtains 99.1% of **III** and 0.9% of combined **I** + **II** at thermal equilibrium in the gas phase.

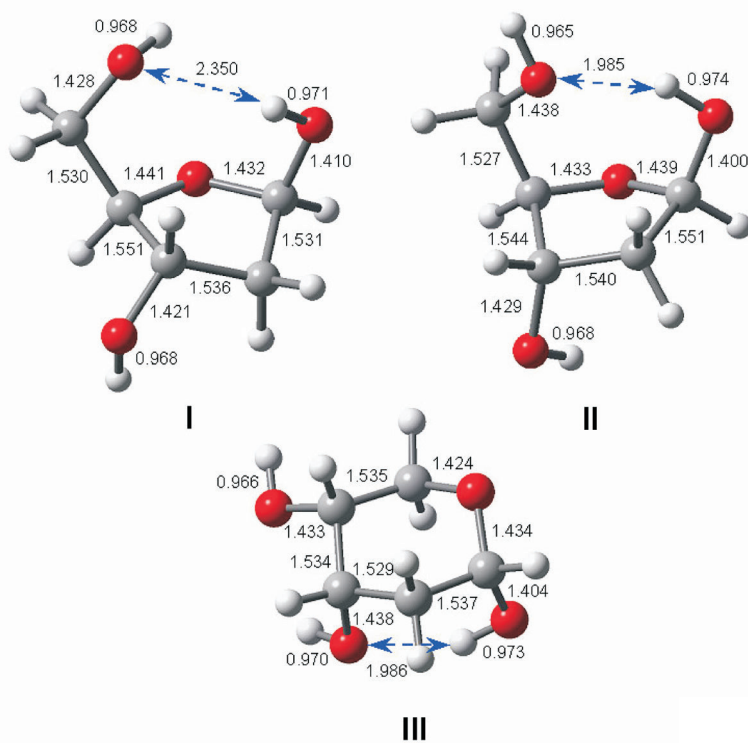


FIG. 1

B3LYP/6-31+G(d,p) optimized geometries of **I–III**. Bond lengths in Å

The free energy differences between the furanose isomers **I**, **II**, and the pyranose isomer **III** are substantially diminished in aqueous solution. According to the PCM solvation free energies,  $\Delta G^{\circ}_{\text{solv}} = -83$ ,  $-79$ , and  $-70$  kJ mol<sup>-1</sup> for **I**, **II**, and **III**, respectively, the corresponding relative free energies in aqueous solution,  $\Delta G^{\circ}_{\text{aq},298}$ , are calculated as  $\Delta G^{\circ}_{\text{aq},298}(\text{I} \rightarrow \text{III}) = 0.4$  kJ mol<sup>-1</sup> and  $\Delta G^{\circ}_{\text{aq},298}(\text{II} \rightarrow \text{III}) = -4.3$  kJ mol<sup>-1</sup>. These indicate that aqueous 2-deoxyribose may exist as a 58:42 mixture of furanose and pyranose structures.

Radical attack on **I** or **II** is presumed to result in hydrogen atom abstraction. The reactivity of the C-H and O-H bonds can be characterized by the relevant bond dissociation energies (BDE) that are summarized in Table I for the most stable radical conformers. This shows that the C-H bonds alpha to the hydroxy groups on C-3, C-4, and C-5 have the lowest dissociation energies, followed by the C-1-H and C-2-H bonds. Predictably, the O-H bonds are stronger than the C-H bonds, but show very similar BDE for O-1-H through O-5-H. The difference between the dissociation free energies of the O-H and C-H bonds is further increased in aqueous solution due to the more efficient solvation of carbon-centered radicals, as discussed below.

TABLE I  
Bond dissociation energies (kJ mol<sup>-1</sup>) in 2-deoxyribofuranose  ${}^2E$  conformer **I**<sup>a</sup>

Bond	B3LYP		B3-PMP2		
	6-31+G(d,p)	6-311+G(2df,p)	6-311++G(3df,2p)	$\Delta G^{\circ}_{\text{diss,g}}$ <sup>b</sup>	$\Delta G^{\circ}_{\text{diss,aq}}$ <sup>c</sup>
C-1-H	387	382	384	346	362
C-2-H	399	395	397	364	383
C-3-H	378	392	378	343	366
C-4-H	378	376	379	340	349
C-5-H	375	370	372	339	360
O-1-H	414	425	429	396	423
O-3-H	417	429	433	400	429
O-5-H	415	432	435	404	440

<sup>a</sup> Including B3LYP/6-31+G(d,p) zero-point vibrational energies and 298 K enthalpies and referring to 298 K. <sup>b</sup> Free energies for bond dissociations in the gas phase at 298 K. <sup>c</sup> Free energies for bond dissociations in water at 298 K.

The gas-phase BDE in **I** are now compared to the hydrogen atom affinities ( $\Delta H_{\text{aff}}$ ) of reactive radicals that are known or thought to be important in radiation and oxidative damage of DNA and proteins. The high hydrogen atom affinity of the OH radical ( $\Delta H_{\text{aff}} = 498 \text{ kJ mol}^{-1}$ )<sup>20</sup> makes all hydrogen atoms in **I** susceptible to exothermic abstraction. Attack at **I** by OH is therefore expected to be non-selective. By contrast, the BDE for the hydrogen atoms in **I** are uniformly greater than the hydrogen atom affinity of the peroxy radical, ( $\text{HOO}^\bullet$ ,  $\Delta H_{\text{aff}} = 367 \text{ kJ mol}^{-1}$ )<sup>21</sup>, making H-atom abstraction by  $\text{HOO}^\bullet$  endothermic. An attack by the reactive N-H iminyl radical generated by H-atom abstraction from the adenine amino group ( $\Delta H_{\text{aff}} = 415 \text{ kJ mol}^{-1}$ )<sup>22</sup> is exothermic only when concerning the C-H bonds in **I**, and can be expected to exhibit some selectivity. Likewise, S-cysteyl, O-tyrosyl, or  $\text{C}_\alpha$ -glycyl radical centers<sup>23</sup> in oxidatively damaged proteins have  $\Delta H_{\text{aff}}$  in the range of 350–367  $\text{kJ mol}^{-1}$ , approaching the BDE of the weakest C-5-H bond in **I** (372  $\text{kJ mol}^{-1}$ ), and may result in H-atom abstraction.

### 2-Deoxyribofuranose Radicals

The relative stabilities of deoxyribose radicals **1–9** in the gas phase and aqueous solution depend on both the position of the radical center and the ring and substituent conformation. The O-1, O-3, and O-5 hydroxy groups and the C-5 methylene introduce four degrees of freedom for internal rotation that result in a total of  $3^4 = 81$  theoretical staggered conformations for each substituent. The gas-phase structures are discussed first. The O-1 hydroxy group greatly prefers the conformation in which the positive end of the O-1-H dipole is oriented toward the furanose ring oxygen atom (O-6)<sup>8</sup>. Likewise, the O-3 hydroxy group prefers conformations that minimize the dipole-dipole interactions between the O-1-H proton and the hydrogen atoms at C-2 and C-3.

Radical **1a** (Fig. 2) assumes a C-2-*endo* (<sup>2</sup>*E*) ring conformation with O-5 pointing toward *endo*-C-2-H. This conformation is only slightly less stable than the C-4-*endo* (<sup>4</sup>*E*) conformation in **1b** that shows a weak hydrogen bond between O-5-H and the ring oxygen atom at a 2.650 Å distance. The third conformer (**1c**, <sup>4</sup>/<sub>3</sub>*T*) has a twisted conformation in which the C-5-O-5 dipole aligns with the C-3-H-3-*endo* dipole. The conformational effects on the conformer relative stabilities are minor for C-1 radicals and do not exceed 6  $\text{kJ mol}^{-1}$  (Table II).

Larger effects are found for the C-2-centered radicals **2a–2c** which prefer envelope ring conformations. The most stable conformer in this group, **2b** (<sup>4</sup>*E*), has the O-5-H bond pointing towards the ring oxygen atom O-6 at a

2.759 Å distance (Fig. 2). The other two rotamers, **2a** ( ${}^3E$ ) and **2c** ( ${}^4E$ ), lack this attractive dipole-dipole interaction and are destabilized by 21 and 11 kJ mol $^{-1}$ , respectively, relative to **2b**.

The C-3-centered radicals **3a** and **3b** have envelope ring conformations ( ${}^1E$  and  ${}^2E$ , respectively), that are enforced by hydrogen bonding involving the O-5 hydroxy group. In **3a**, the O-5-H proton forms a hydrogen bond to

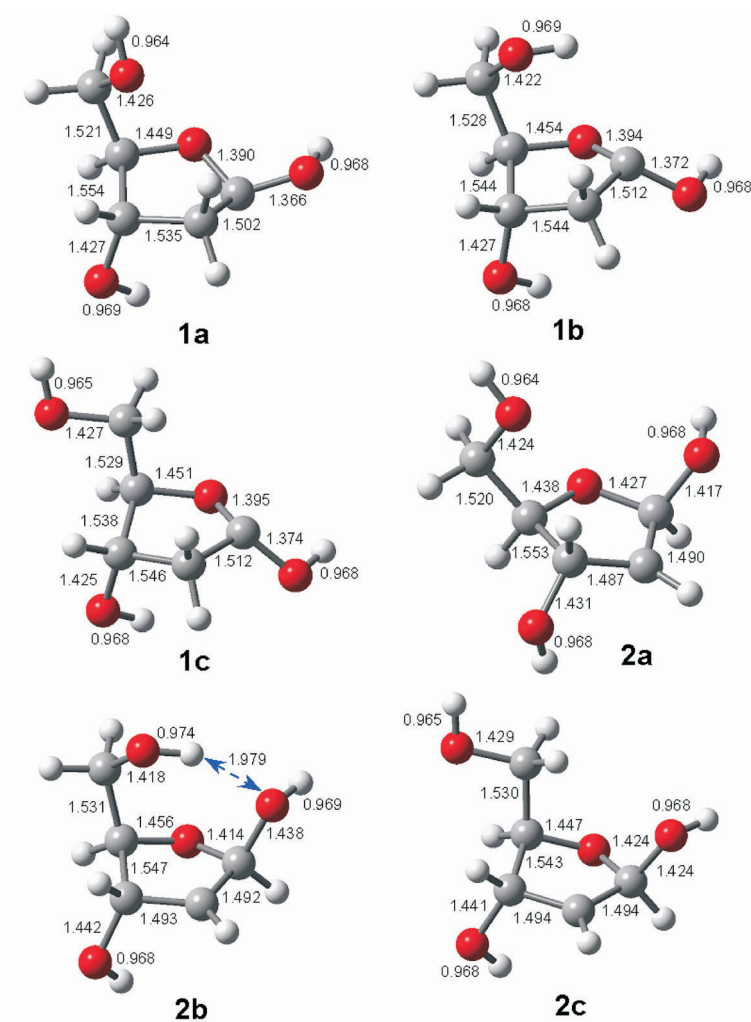


FIG. 2  
B3LYP/6-31+G(d,p) optimized geometries of **1a-1c** and **2a-2c**. Bond lengths in Å

O-1 at a 2.058 Å distance. This conformation is 13 kJ mol<sup>-1</sup> more favorable than that in **3b**, which shows a hydrogen bond between O-3-H and O-5 at a 2.189 Å distance (Fig. 3).

Effects of C-5 and O-5 conformations are diminished in the C-4-centered radicals **4a** and **4b** that both have C-2-*exo* (<sub>2</sub>*E*) ring conformations in which the furanose ring is flattened at C-4 due to its sp<sup>2</sup> hybridization (Fig. 3). **4b** is the second most stable radical overall while **4a** is only 5 kJ mol<sup>-1</sup> less stable than **4b** (Table II).

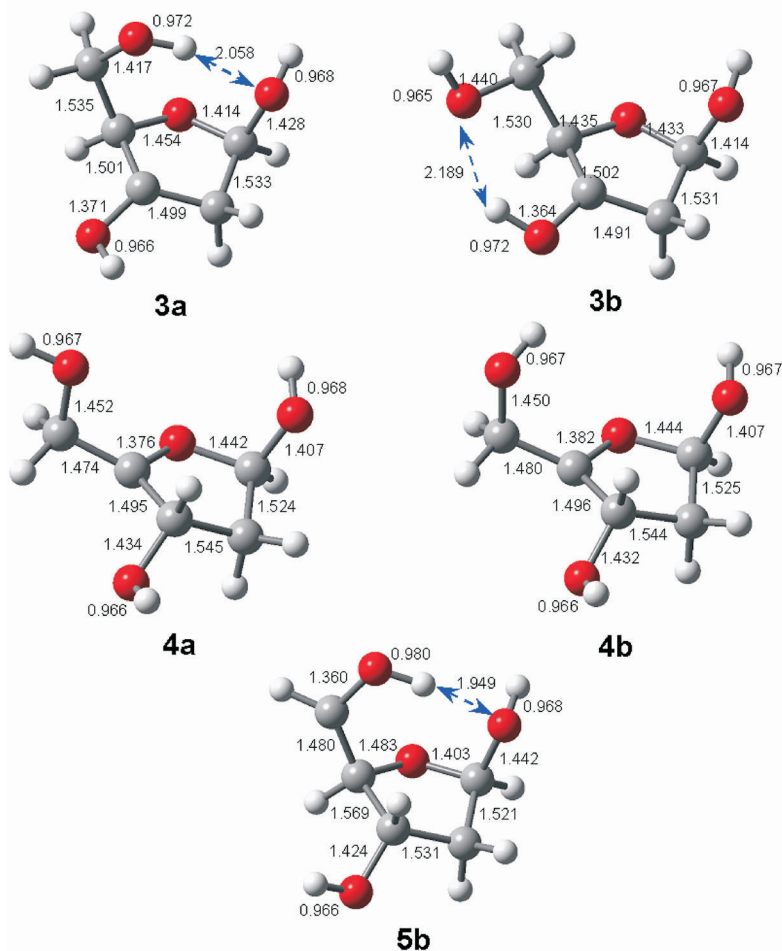


FIG. 3  
B3LYP/6-31+G(d,p) optimized geometries of **3a**, **3b**, **4a**, **4b**, and **5**. Bond lengths in Å



Out of the C-5-centered radicals, **5b** is the global energy minimum of the present set. This stability is mainly due to the hydrogen bond between O-5-H and O-1 at a 1.949 Å distance and the favorable alignment of the O-5-H bond dipole with those of the ring C-O bonds (Fig. 3). It is not immediately clear whether the  $sp^2$ -hybridized C-5 has any significant electronic effect on stabilizing **5b** relative to the C-3 and C-4-centered radicals. In any case, the energy differences between the most stable C-5, C-4, and C-3 radical conformers are small, indeed ( $\leq 8$  kJ mol<sup>-1</sup>, Table II).

Finally, hydrogen bonding plays a role in determining the stable conformations of the oxygen-centered radicals **7-9**. The O-1-centered radical **7** (<sup>4</sup>E) shows a hydrogen bond between O-1 and the O-5-H hydroxy group at

TABLE II  
Relative energies (kJ mol<sup>-1</sup>) of 2-deoxyribofuranose radicals<sup>a</sup>

Species	B3LYP	B3-PMP2 <sup>b</sup>		$\Delta G_{\text{solv}}^c$
	6-31+G(d,p)	6-311+G(2df,p)	6-311++G(3df,2p)	
<b>1a</b>	14	13(0.6)	13(0.6)	-86
<b>1b</b>	11	11(2)	10(2)	-81
<b>1c</b>	17	17(3.5)		-86
<b>2a</b>	45	46(17)		-98
<b>2b</b>	24	25(22)	25(23)	-78
<b>2c</b>	36	36(18)		-91
<b>3a</b>	20	7(1)	7(1)	-81
<b>3b</b>	6	3(4)	5(6)	-74
<b>4a</b>	5	9(-10)	9(-10)	-90
<b>4b</b>	0.6	4(-12)	4(-11)	-88
<b>5a</b>	13	12(-8)	12(-8)	-94
<b>5b</b>	0	0(0)	0(0)	-76
<b>7</b>	40	56(62)	57(63)	-70
<b>8</b>	42	59(67)	61(69)	-68
<b>9a</b>	53	80(80)	69(69)	-75
<b>9b</b>	41	63(80)	63(80)	-61

<sup>a</sup> Including B3LYP/6-31+G(d,p) zero-point energies and referring to the gas phase at 0 K.

<sup>b</sup> Relative free energies in water at 298 K are given in parentheses. <sup>c</sup> Solvation free energies at 298 K from PCM/B3LYP/6-31+G(d,p) optimizations.

a 2.140 Å distance (Fig. 4). Radical **8** has a twisted ring conformation ( $\frac{1}{2}T$ ) and its O-1-H bond is *endo*-oriented toward O-5 at a 2.308 Å distance. The O-5 centered radical **9** ( $^4E$ ) shows a regular hydrogen bond between O-5 and O-1-H at a 1.953 Å distance. The relative stabilities of **7–9** are similar being within 57–63 kJ mol<sup>-1</sup> of **5b**.

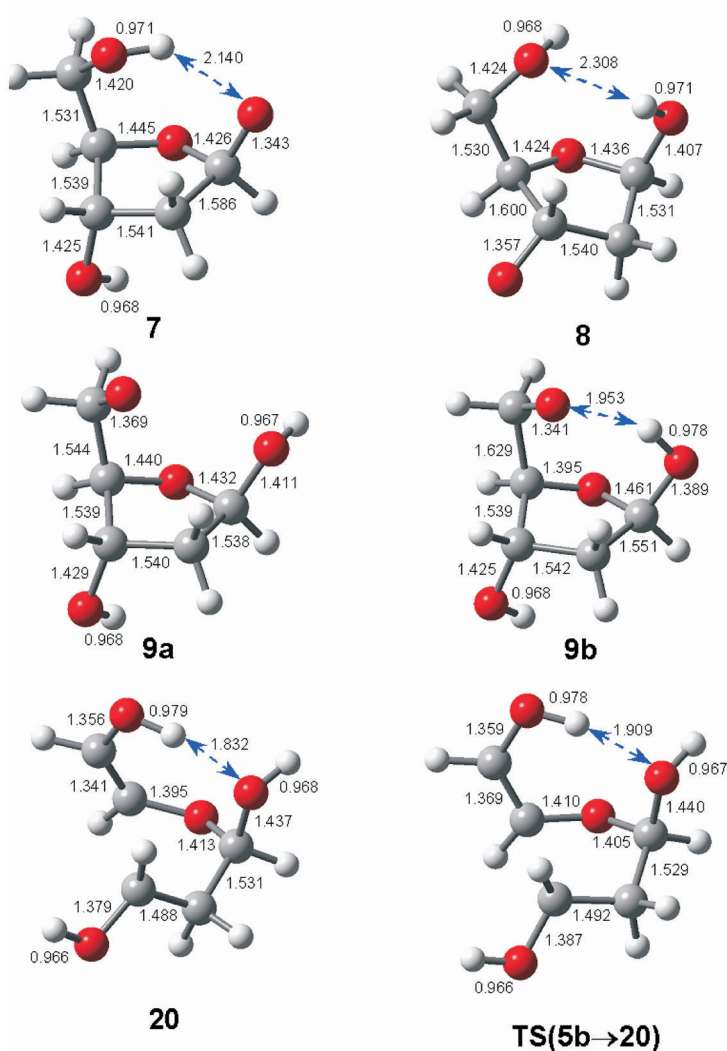


FIG. 4  
B3LYP/6-31+G(d,p) optimized geometries of **7**, **8**, **9a**, **9b**, **20**, and **TS(5b→20)**

### *Solvent Effects on Radical Stabilities*

Owing to the narrow range of radical relative energies in the gas phase, the order of relative stabilities of **1–9** is greatly affected by solvent effects (Table II). The PCM solvation free energies for **1–9** fall within the range from  $-61$  to  $-91$  kJ mol<sup>-1</sup> (Table II). Solvation mainly affects the O–H bond lengths that are generally 0.02 Å longer in the structures optimized in the water dielectric compared to the gas-phase ones. The largest stabilization is observed for conformers that do not show strong intramolecular hydrogen bonds and expose the O–H bonds to the solvent, e.g., in **2a**, **4a**, and **5a**. In contrast, oxygen-centered radicals **7–9** that lack one O–H bond show less stabilization by solvent effects (Table II). The radical relative free energies in solution point to **4b**, **4a**, and **5a** as the most stable structures, followed by the C-1-centered radicals **1a**, **1b**, and the C-3-centered ones **3a**, **3b**. It should be noted that the free energy differences among these isomers are small and well within the accuracy of the PCM model, and thus the relative ordering of the radical stabilities may depend on the type of theoretical model describing the solvation.

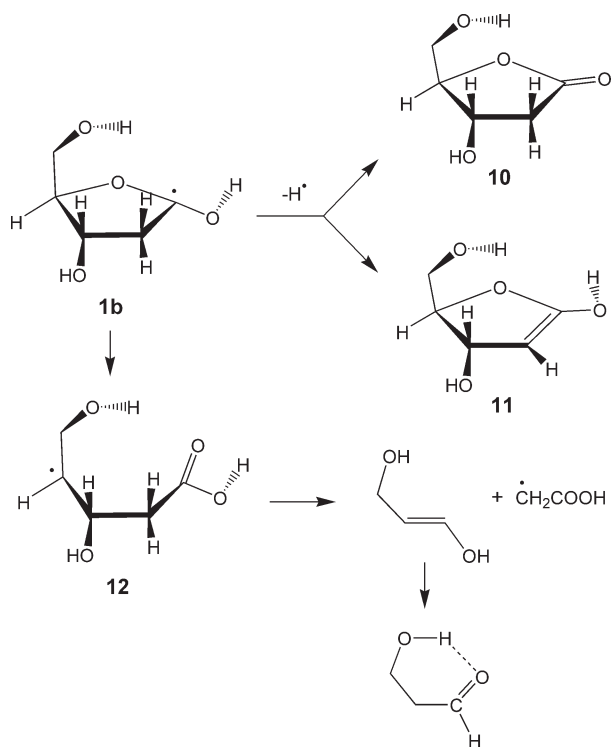
### *Dissociation Energetics of 1–9*

In addition to the structures and relative stabilities of deoxyribose radicals **1–9**, we also address the energetics of their dissociations by loss of H atoms, OH radicals, and C–C bond cleavages. Of particular interest are the dissociation energies and the nature of the saccharide products.

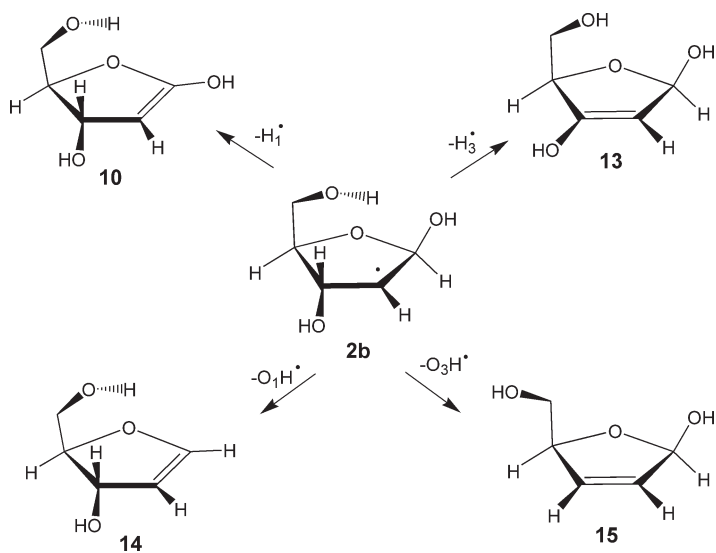
Radicals **1** (either conformer) can dissociate by eliminating a hydrogen atom from the positions adjacent to C-1 (Scheme 1). Elimination of H from O-1 produces 2-deoxyribo-1-lactone (**10**) at 37 kJ mol<sup>-1</sup> threshold energy from **1b** (Table III). The O-1–H bond dissociation probably requires a higher energy in the transition state ( $\sim 90$  kJ mol<sup>-1</sup>), as judged by the analogous dissociation in 2-hydroxytetrahydrofuran-2-yl radical<sup>8</sup>.

Dissociation of one of the C-2–H bonds would produce enol **11** at 127 kJ mol<sup>-1</sup> threshold energy from **1b**. Although we did not study ring cleavages in **1b**, previous calculations with 2-hydroxytetrahydrofuran-2-yl radical indicate that the C-4–O-6 bond can be expected to be particularly weak and break with a  $\sim 50$  kJ mol<sup>-1</sup> activation energy to give radical **12**. The latter can further dissociate to  $\cdot\text{CH}_2\text{COOH}$  and the enol of 3-hydroxypropanal (Scheme 1), or undergo isomerizations by hydrogen atom migrations.

The C-2 radical center in **2b** can activate the C–H, C–O, and C–C bonds at the adjacent atoms to trigger loss of H, OH, or ring cleavage (Scheme 2).



SCHEME 1



SCHEME 2

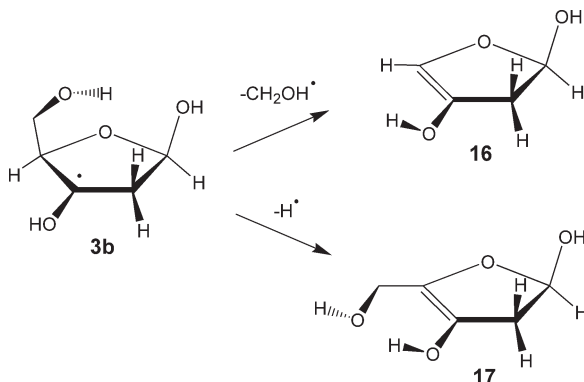
Losses of H from C-1 or C-3 in **2b** show very similar threshold energies, 113 and 110 kJ mol<sup>-1</sup>, respectively. These dissociations probably require transition state energies of 30–40 kJ mol<sup>-1</sup> in excess of the BDE, by analogy with C–H bond dissociations in other radical systems<sup>8</sup>. The eliminations of OH from **2b** show different threshold energies for 1-OH (146 kJ mol<sup>-1</sup>) and 3-OH (121 kJ mol<sup>-1</sup>). Since OH additions to double bonds usually have very low activation energies, the BDE for C–O in **2b** are close approximations of the activation energies for OH loss. Interestingly, loss of 3-OH forming the 2,5-dihydrofuran derivative **15** requires less energy than loss of 1-OH forming the 1,2-dihydrofuran **14** (Scheme 2).

TABLE III  
Dissociation energies (kJ mol<sup>-1</sup>) in 2-deoxyribofuranose radicals<sup>a</sup>

Reaction	B3LYP	B3-PMP2	
	6-31+G(d,p)	6-311+G(2df,p)	6-311++G(3df,2p)
<b>1b</b> → <b>10</b> + H <sup>•</sup>	58	34	37
<b>1b</b> → <b>11</b> + H <sup>•</sup>	149	124	127
<b>2b</b> → <b>10</b> + H <sup>•</sup>	136	111	113
<b>2b</b> → <b>13</b> + H <sup>•</sup>	133	107	110
<b>2b</b> → <b>14</b> + OH <sup>•</sup>	138	144	146
<b>2b</b> → <b>15</b> + OH <sup>•</sup>	114	118	121
<b>3b</b> → <b>16</b> + <sup>•</sup> CH <sub>2</sub> OH	100	85	102
<b>3b</b> → <b>17</b> + H <sup>•</sup>	160	119	140
<b>4b</b> → <b>17</b> + H <sup>•</sup>	170	144	148
<b>4b</b> → <b>18</b> + OH <sup>•</sup>	125	129	131
<b>4b</b> → <b>19</b> + OH <sup>•</sup>	123	126	128
<b>5b</b> → TS( <b>5b</b> ) → <b>20</b> )	99	105	106
<b>5b</b> → <b>20</b>	81	85	86
<b>8</b> → TS( <b>8</b> → <b>22</b> )	26	21	22
<b>8</b> → <b>22</b>	6	-0.5	-0.5
<b>9b</b> → <b>24</b> + CH <sub>2</sub> O	26	14	14

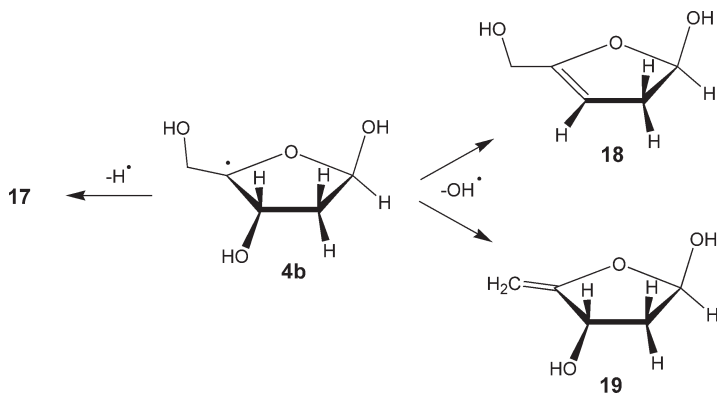
<sup>a</sup> Including B3LYP/6-31+G(d,p) zero-point energies and referring to 0 K in the gas phase.

The C-3 radical center can also activate the adjacent bonds for dissociation. Scheme 3 shows the loss of the CH<sub>2</sub>OH group producing enol **16** at 102 kJ mol<sup>-1</sup> threshold energy, and loss of H-3 yielding enol **17** at 140 kJ mol<sup>-1</sup>.



SCHEME 3

Dissociations of the C-4-centered radical **4b** can involve a loss of H-3 forming enol **17**, and eliminations of the O-5 and O-5 hydroxy groups forming products **18** and **19**, respectively (Scheme 4). The latter two dissociations show very similar threshold energies, 131 and 128 kJ mol<sup>-1</sup>, respectively, and can be expected to be kinetically competitive.

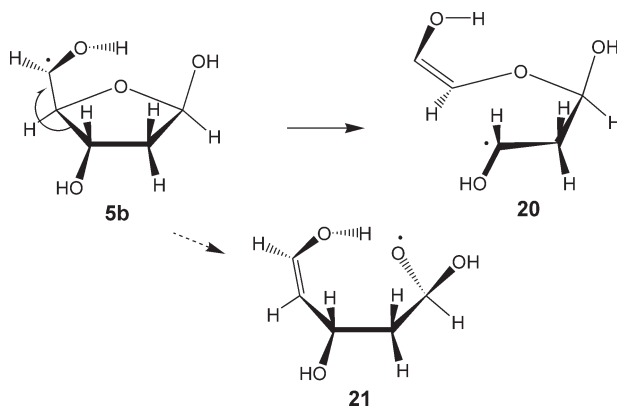


SCHEME 4

The radical center at C-5 can activate the C-4-H, C-4-C-3, and C-4-O-6 bonds. In particular, we studied the dissociation of the C-4-C-3 bond (Scheme 5) that results in ring opening and formation of intermediate **20** (Scheme 5). The bond cleavage requires 106 kJ mol<sup>-1</sup> in the transition state and is overall 86 kJ mol<sup>-1</sup> endothermic. The alternative dissociation of the

C-4-O-6 bond would form a high-energy O-6-centered radical (**21**) that was not considered to be competitive with the C-4-C-3 bond dissociation.

The oxygen-centered radicals **8** and **9b** show very low dissociation energies for cleavages of bonds that are adjacent to the radical center. In **8**, a ring opening by cleavage of the C-3-C-4 bond is nearly thermoneutral to



SCHEME 5

form radical **22** that requires only 22 kJ mol<sup>-1</sup> in the transition state, TS(**8**→**22**). The stabilization of the transition state (TS) and **22** comes in part from the stronger hydrogen bond between O-1-H and O-5 as evidenced by the shortened H...O-5 distance from 2.308 Å in **8** to 1.862 Å in TS(**8**→**22**) and 1.799 Å in **22** (Fig. 5). This hydrogen bond shortening is

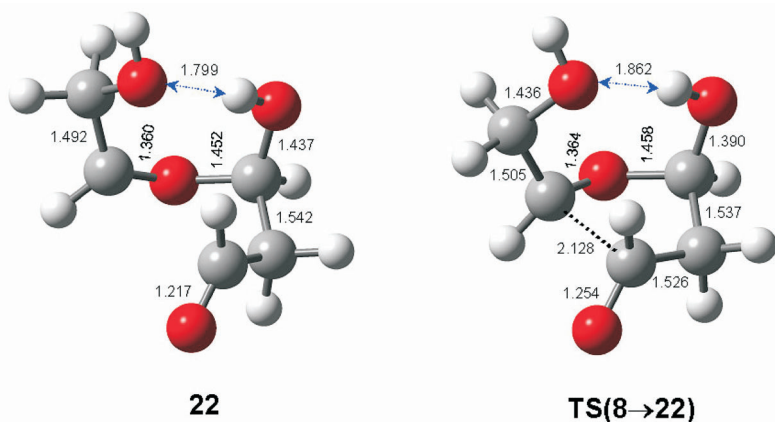
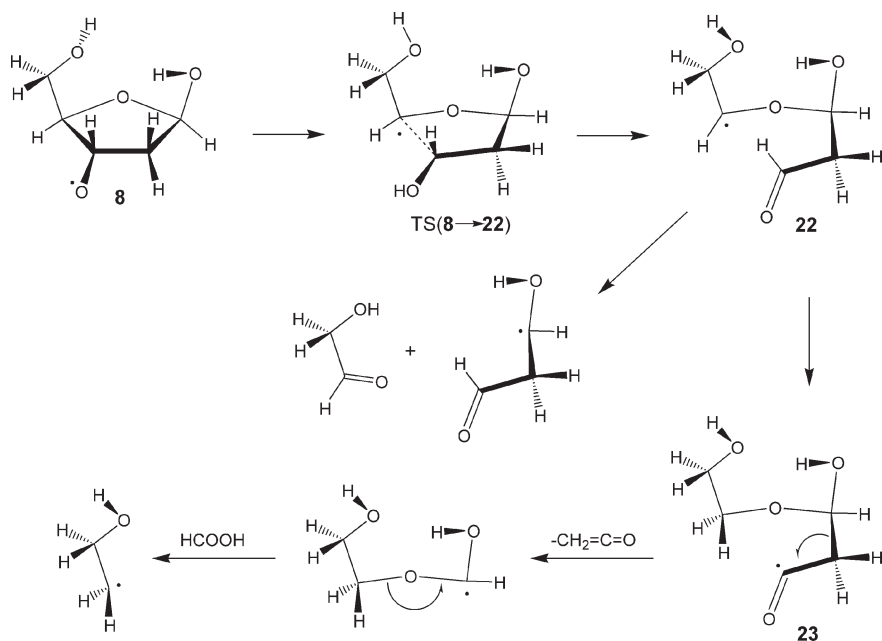


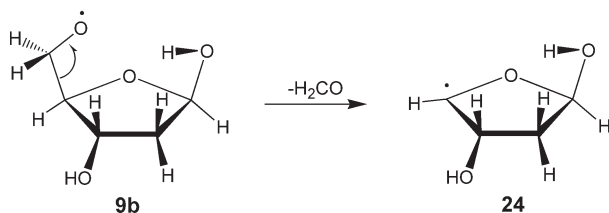
FIG. 5  
B3LYP/6-31+G(d,p) optimized geometries of **22** and TS(**8**→**22**)

made possible by the increased flexibility of the furanose skeleton as the C-3-C-4 bond is interrupted.

Further reactions of intermediate **22** may involve fragmentation to glycolaldehyde and a hydroxypropanal radical, or intramolecular hydrogen transfer forming **23**, followed by fragmentation by elimination of ketene (Scheme 6). Radical **9b** is calculated to undergo a very facile dissociation of the C-4-C-5 bond to lose formaldehyde forming nor-5 radical **24** (Scheme 7). This dissociation requires only 14 kJ mol<sup>-1</sup> at the thermochemical threshold (Table III) and is expected to have a low activation energy.



SCHEME 6



SCHEME 7



In summary, oxygen-centered 2-deoxyribofuranose radicals are energetically accessible by hydrogen atom abstraction from the parent saccharide molecule by OH radical and show only marginal stability. Dissociations can be initiated by ring cleavage followed by fragmentations in the intermediates or by losses of substituents. Carbon-centered radicals are energetically accessible by H-atom abstraction with a variety of organic radicals, namely, adenyl, tyrosyl, and cysteyl radicals. The H-atom abstraction from 2-deoxyribose by these radicals is predicted to show some selectivity in affecting the most reactive positions C-3 through C-5. Dissociations of carbon-centered 2-deoxyribofuranose radicals as a rule require transition state or dissociation energies exceeding  $100 \text{ kJ mol}^{-1}$ . Of the dissociations studied here, loss or transfer of H atoms and OH radicals show very similar threshold energies suggesting several competitive dissociation channels. These findings are consistent with previous experimental studies of saccharide radiolysis that resulted in largely non-specific formation of a number of dissociation products<sup>24</sup>. One interesting finding of the present study is that H-atom abstraction from 2-deoxyribofuranose by the peroxy radical is endothermic and may render the DNA backbone immune to oxidative attack by  $\cdot\text{OOH}$ .

*Generous support of this work by the National Science Foundation (Grants CHE-0349595 and CHE-0342956) is gratefully acknowledged.*

## REFERENCES

1. Becker D., Sevilla M. D. in: *Advances in Radiation Biology* (J. T. Lett and W. K. Sinclair, Eds), Vol. XVII, p. 121. Academic Press, San Diego 1993.
2. Von Sonntag C.: *Adv. Carbohydr. Chem. Biochem.* **1980**, 37, 7.
3. a) Close D. M.: *Radiat. Res.* **1997**, 148, 512; b) Close D. M.: *Radiat. Res.* **1997**, 147, 663.
4. Miaskiewicz K., Osman R.: *J. Am. Chem. Soc.* **1994**, 116, 232.
5. Colson A.-O., Sevilla M. D.: *J. Phys. Chem.* **1995**, 99, 3867.
6. Wetmore S. D., Boyd R. J., Eriksson L. A.: *J. Phys. Chem. B* **1998**, 102, 7674.
7. a) Altona C., Sundaralingam M.: *J. Am. Chem. Soc.* **1972**, 94, 8205; b) Arnott S., Hukins D. W. L.: *Biochem. J.* **1972**, 130, 453.
8. Vivekananda S., Sadílek M., Chen X., Tureček F.: *J. Am. Soc. Mass Spectrom.* **2004**, 15, 1055.
9. Vivekananda S., Sadílek M., Chen X., Adams L. E., Tureček F.: *J. Am. Soc. Mass Spectrom.* **2004**, 15, 1068.
10. Furberg S.: *Acta Chem. Scand.* **1960**, 14, 1357.
11. Frisch M. J., Trucks G. W., Schlegel H. B., Scuseria G. E., Robb M. A., Cheeseman J. R., Montgomery J. A., Jr., Vreven T., Kudin K. N., Burant J. C., Millam J. M., Iyengar S. S., Tomasi J., Barone V., Mennucci B., Cossi M., Scalmani G., Rega N., Petersson G. A.,

- Nakatsuji H., Hada M., Ehara M., Toyota K., Fukuda R., Hasegawa J., Ishida M., Nakajima T., Honda Y., Kitao O., Nakai H., Klene M., Li X., Knox J. E., Hratchian H. P., Cross J. B., Adamo C., Jaramillo J., Gomperts R., Stratmann R. E., Yazyev O., Austin A. J., Cammi R., Pomelli C., Ochterski J. W., Ayala P. Y., Morokuma K., Voth G. A., Salvador P., Dannenberg J. J., Zakrzewski V. G., Dapprich S., Daniels A. D., Strain M. C., Farkas O., Malick D. K., Rabuck A. D., Raghavachari K., Foresman J. B., Ortiz J. V., Cui Q., Baboul A. G., Clifford S., Cioslowski J., Stefanov B. B., Liu G., Liashenko A., Piskorz P., Komaromi I., Martin R. L., Fox D. J., Keith T., Al-Laham M. A., Peng C. Y., Nanayakkara A., Challacombe M., Gill P. M. W., Johnson B., Chen W., Wong M. W., Gonzalez C., Pople J. A.: *Gaussian 03*, Revision B.05. Gaussian, Inc., Pittsburgh (PA) 2003.
12. a) Becke A. D.: *J. Chem. Phys.* **1993**, *98*, 1372; b) Becke A. D.: *J. Chem. Phys.* **1993**, *98*, 5648; c) Stephens P. J., Devlin F. J., Chabalowski C. F., Frisch M. J.: *J. Phys. Chem.* **1994**, *98*, 11623.
13. Møller C., Plesset M. S.: *Phys. Rev.* **1934**, *46*, 618.
14. a) Mayer I.: *Adv. Quantum Chem.* **1980**, *12*, 189; b) Schlegel H. B.: *J. Chem. Phys.* **1986**, *84*, 4530.
15. Tureček F.: *J. Phys. Chem. A* **1998**, *102*, 4703.
16. a) Tureček F., Wolken J. K.: *J. Phys. Chem. A* **1999**, *103*, 1905; b) Tureček F., Wolken J. K., Sadílek M.: *Eur. Mass Spectrom.* **1998**, *4*, 321; c) Wolken J. K., Tureček F.: *J. Am. Chem. Soc.* **1999**, *121*, 6010; d) Wolken J. K., Tureček F.: *J. Phys. Chem. A* **1999**, *103*, 6268; e) Tureček F., Carpenter F. H.: *J. Chem. Soc., Perkin Trans. 2* **1999**, 2315; f) Polášek M., Tureček F.: *J. Am. Chem. Soc.* **2000**, *122*, 9511.
17. a) Rablen P. R.: *J. Am. Chem. Soc.* **2000**, *122*, 357; b) Rablen P. R., Bentrup K. H.: *J. Am. Chem. Soc.* **2003**, *125*, 2142.
18. a) Cossi M., Scalmani G., Rega N., Barone V.: *J. Chem. Phys.* **2002**, *117*, 43; b) Cossi M., Scalmani G., Rega N., Barone V.: *Biochemistry* **1999**, *38*, 9089.
19. Gia H., Garrett B. C.: *J. Phys. Chem.* **1994**, *98*, 9642.
20. Ruscic B., Wagner A. F., Harding L. B., Asher R. L., Feller D., Dixon D. A., Peterson K. A., Song Y., Qian X., Ng C.-Y., Liu J., Chen W., Schwenke D. W.: *J. Phys. Chem. A* **2002**, *106*, 2727.
21. Ramond T. M., Blanksby S. J., Kato S., Bierbaum V. M., Davico G. E., Schwartz R. L., Lineberger W. C., Ellison G. B.: *J. Phys. Chem. A* **2002**, *106*, 9641.
22. Chen X., Syrstad E. A., Gerbaux P., Nguyen M. T., Tureček F.: *J. Phys. Chem. A* **2004**, *108*, 9283.
23. a) Rauk A., Yu D., Armstrong D. A.: *J. Am. Chem. Soc.* **1998**, *120*, 8848; b) Rauk A., Yu D., Taylor J., Shustov G. V., Block D. A., Armstrong D. A.: *Biochemistry* **1999**, *38*, 9089.
24. Kochetkov N. K.: *Radiation Chemistry of Carbohydrates*. Pergamon Press, Oxford 1979.